



# An enhanced planned obsolescence attack by aging networks-on-chip<sup>☆</sup>

Yinyuan Zhao<sup>a</sup>, Xiaohang Wang<sup>a,b,\*</sup>, Yingtao Jiang<sup>c</sup>, Liang Wang<sup>d</sup>, Amit Kumar Singh<sup>e</sup>,  
Letian Huang<sup>f</sup>, Mei Yang<sup>c</sup>

<sup>a</sup> School of Software Engineering, South China University of Technology, Guangzhou, China

<sup>b</sup> State Key Laboratory of Computer Architecture, Institute of Computing Technology, Chinese Academy of Sciences, Beijing, China

<sup>c</sup> Department of Electrical and Computer Engineering, University of Nevada, Las Vegas, USA

<sup>d</sup> School of Computer Science and Engineering, Beihang University, Beijing, China

<sup>e</sup> School of Computer Science and Electronic Engineering, University of Essex, Colchester, UK

<sup>f</sup> University of Electronic Science and Technology of China, Chengdu, China

## ARTICLE INFO

### Keywords:

Planned obsolescence

Aging

Networks-on-chip (NoCs)

## ABSTRACT

Despite of a controversial practice, having the key components of a product undergo accelerated aging has been a very effective approach for planned obsolescence. All previous studies on planned obsolescence merely focused on the aging process itself; however, if a malfunctioned product due to aging is still under its warranty, the manufacturer suffers from financial losses in the form of customer refund and/or product repair. In this paper, we reveal an enhanced planned obsolescence attack that takes the warranty issue into consideration. More specifically, aging of an NoC-based many-core chip is set to be slow before the warranty expires, and its aging process gets accelerated afterwards. Such controlled aging is achieved by manipulating the routing algorithm that influences the lifetime distribution of the NoC nodes. The routing-induced aging process is also integrated with a profit model to evaluate the profit gained from chip aging. Experimental results show that, with the proposed planned obsolescence attack and the profit model, the manufacturer can increase its profit margin by 15.54%, 25.69%, and 53.36%, respectively, compared to devices under a scheme without any attack, a scheme that aggressively accelerates chip aging, and a scheme that employs a measure to mitigate chip aging. Overall speaking, the proposed attack can give the manufacturer a clear advantage over customer who can barely notice the existence of such business practices, and consequently, some advanced countermeasure schemes need to be developed to balance the interests of the two parties.

## 1. Introduction

Planned obsolescence in industrial design and marketing is a notorious strategy to deliberately set product to malfunction within a certain period of time [1]. Quite a few consumer electronics vendors have been reported of engaging in such practice of obsolescence by downgrading their old products to drive customers to move to their newer versions of products [1].

A manufacturer often favors this type of obsolescence by either deliberately crafting malicious programs or inserting hardware backdoors that can be exploited to accelerate aging of key components, such as cores and some of the critical links in many-core chips [1,2]. For

many-core systems connected by networks-on-chip (NoCs), aging the interconnection is more destructive than wearing out the cores [3,4]. A fault in one core might not result in failure of the entire chip, as the problem can be tackled by scheduling the affected tasks to other fault-free cores to take advantage of high degree of redundancy in a many-core chip. However, the malfunction of key component in NoCs, like a critical router which carries most traffic or connects to the memory controllers, may render the whole system faulty, even though each core may still be working as expected. Up to date, there are few research works tackling planned obsolescence attacks on NoC routers [1,2]. The work presented in this paper thus attempts to study

<sup>☆</sup> This research program was supported in part by the National Natural Science Foundation of China under Grant 61971200, in part by the Natural Science Foundation of Guangdong Province, China under Grant 2018A030313166, in part by Pearl River S&T Nova Program of Guangzhou, China under Grant 201806010038, in part by Fundamental Research Funds for the Central Universities, China under Grant 2019MS087, in part by Open Research Grant of State Key Laboratory of Computer Architecture Institute of Computing Technology Chinese Academy of Sciences under Grant CARCH201916, in part by Key Laboratory of Big Data and Intelligent Robot (South China University of Technology), Ministry of Education, in part by Zhejiang Lab under Grant 2021LE0AB01, in part by National Key Research and Development Program of China under Grant 2019QY0705.

\* Corresponding author.

E-mail address: [xiaohangwang@scut.edu.cn](mailto:xiaohangwang@scut.edu.cn) (X. Wang).

<https://doi.org/10.1016/j.sysarc.2021.102093>

Received 29 October 2020; Received in revised form 28 January 2021; Accepted 9 March 2021

Available online 13 March 2021

1383-7621/© 2021 Elsevier B.V. All rights reserved.

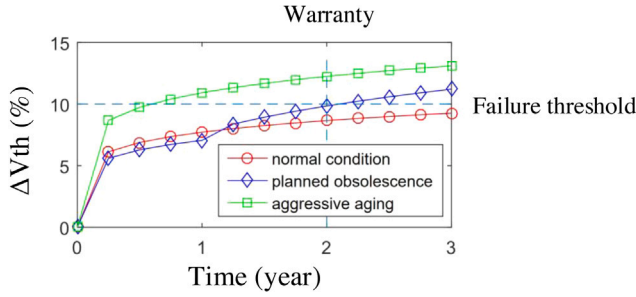


Fig. 1. Different scenarios of aging.

such attacks from the viewpoint of the most critical routers in NoC, the so-called hotspot nodes.

Targeting a hotspot node and making it age faster can certainly cause a product to obsolete fast. However, if the chip wears out before its warranty expires, the manufacturer is obligated to refund consumers or replace/repair the product, which undermines the purpose of planned obsolescence. In a simple word, blindly accelerating aging does not serve the best interest of the manufacturer. Instead, manufacturer prefers to have its component/product work perfectly at the customer end when it is still under the warranty, but it would wear out as soon as the warranty expires. Fig. 1 shows the expected behavior of the chips from the manufacturer's perspective. The lifetime of a chip is here determined by the variation of transistor threshold voltage,  $\Delta V_{th}$ , which gradually increases as the aging of the transistors [2]. When  $\Delta V_{th}$  exceeds an acceptable threshold, it may introduce serious timing violations that will cause the chip to malfunction [5]. For a manufacturer, the planned obsolescence curve (the blue curve) is thus preferred, and the aggressive aging curve (the green curve), on the other hand, really hurts the manufacturer by eroding its profitability and reputation.

In this paper, we integrate the planned obsolescence attack with a profit model. We study how the manufacturer can maximize its profit by designing an improved planned obsolescence attack that both exploits the vulnerability of chip aging and considers the warranty period. We target the hotspot nodes among the NoC routers as failure of such a node causes the whole chip to disconnect and malfunction. The routing algorithm is used as the control knob to either accelerate or decelerate aging of NoC due to the stealthiness of the routing algorithm (further analyzed in Section 2.4). With the warranty in mind, the manufacturer sees modest aging process before a specific time as defined by the warranty (further analyzed in Section 5.2.2), the aging process is accelerated after it is past the time threshold.

The contributions of the paper are fourfold.

- A profit model is built to determine the profit of the manufacturer. The variables are drawn from the statistics of questionnaires or random variables.
- The routing algorithms for both aging acceleration and deceleration are proposed. Targeting the vulnerability of NoCs, the proposed algorithms accelerate or decelerate aging while keeping the minimal routing of the packets.
- Experimental results show that the proposed aging acceleration routing algorithm decreases the mean time to failure (MTTF) of the hotspot node by about 47.54%, and the proposed aging deceleration routing algorithm increases the MTTF of the hotspot node by about 18.46%.
- Experimental results show that the profit with the proposed planned obsolescence attack is 15.54%, 25.69%, and 53.36% higher than the normal condition, acceleration only and deceleration only schemes, respectively.

Note that the effects of a planned obsolescence attack launched by the manufacturer can be unnoticed by customers for a long period of time. One major focus of this work is thus to provide an in-depth analysis that will expose such attack to customers who otherwise will be kept in the dark. In possession of this critical knowledge, customers can take all the necessary measures or countermeasures that they are entitled to for the best protection of their interest.

The rest of this paper is organized as follows. Section 2 introduces the preliminaries and reviews the related works. Section 3 describes the manufacturer strategy. The details of the aging acceleration and aging deceleration routing algorithms are described in Section 4. Section 5 evaluates the experimental results. Finally, Section 6 concludes the paper.

## 2. Preliminaries and related work

### 2.1. Device level aging effects

NoC suffers from various device level aging effects, including negative bias temperature instability (NBTI) [6,7], hot carrier injection (HCI) [8,9], and electromigration (EM) [10]. These aging effects cause transistor and/or wire links wear-out.

Negative bias temperature instability (NBTI) manifests an increase in p-type transistor's threshold voltage ( $V_{th}$ ) which can be modeled by [11],

$$\Delta V_{th} = be^{-\frac{nE_a}{kT}} \left( \frac{\alpha}{1-\alpha} \right)^n t^n \quad (1)$$

where  $b$  is a fitting constant,  $n$  is the time exponent,  $E_a$  is the apparent activation energy,  $k$  is the Boltzmann's constant,  $T$  is the run-time temperature,  $\alpha$  is the duty cycle, and  $t$  is the operating time.

A direct consequence of NBTI-induced threshold shift is the decrease in transistor's drain current and transconductance, which introduces extra delay in the critical path [7]. As so, NBTI has been known as the most destructive aging effect upon NoC routers [3].

Hot carrier injection (HCI) in MOSFETs occurs when a carrier from silicon channel is injected into the gate dielectric layer [9], and it can permanently change the switching characteristics of the transistor, including  $V_{th}$  shifting and switching frequency degradation. In general, HCI poses a great reliability challenge to n-type transistors [8].

As the primary aging factor in interconnect wires [3], electromigration (EM) refers to gradual displacement of metal wire atoms. EM can cause open and short circuits and it only gets worse at advanced technology nodes as wires are progressively becoming thinner and accordingly, current densities are higher. As NoCs typically come with a large number of long and thin wires, they are susceptible to EM related aging [10].

### 2.2. Aging at NoCs

It has been shown in [3] that the routers in an NoC age at different paces. Consider a mesh-based NoC that supports XY routing. Routers located at the center of the chip handle more network traffic than other routers. Referred as "hotspot nodes", these centrally located routers tend to experience accelerated aging due to the exponential nature of the NBTI effect, making them the most vulnerable components of the system.

Using Alpha Power Law and the AC stress model given in Eq. (1), the lifetime (measured by mean time to failure, MTTF) of a router is given as [4],

$$MTTF = [b_{NBTI} e^{\frac{nE_a}{kT}} \left( \frac{\alpha}{1-\alpha} \right)^n]^{1/n} \quad (2)$$

where  $b_{NBTI}$  is a fitting constant.

Note that an NoC system's lifetime is bounded by the hotspot node, which is the router with the lowest MTTF [12]. That is, the MTTF of the entire chip system,  $MTTF_{sys}$ , can be written as,

$$MTTF_{sys} = \min_{vi \in [1, N]} MTTF_i \quad (3)$$

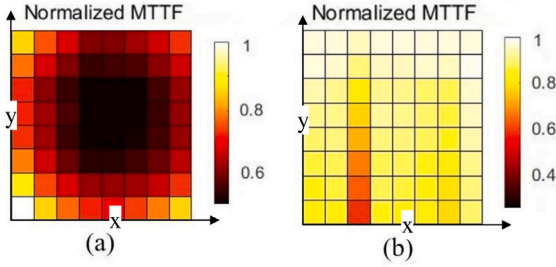


Fig. 2. (a) The hotspot nodes identified as the central routers of NoC and (b) the hotspot nodes identified as the routers directly connected to the memory controller.

where  $N$  is the number of routers.

The normalized MTTF distribution of an  $8 \times 8$  2D mesh network is shown in Fig. 2(a), where one can see that the central routers age at a much higher pace than many other routers. Besides these routers at the central locations, it can also be seen from Fig. 2(b) that for those routers connected to the memory controller, even if they are off the central location, they qualify to become the hotspot nodes as they handle a lot of data traffic from and to the memory, and thus undergo rapid aging as well.

Lifetime and reliability of the routers in an NoC are so such dependent on the underline routing algorithm [12]. Fig. 3 shows the routers' normalized MTTFs of two cases: the NoC adopting deterministic XY routing vs. the NoC adopting adaptive odd-even (OE) routing [13]. In the case of XY routing, the ratio of the highest and lowest MTTFs of the routers is 2:1, while this ratio jumps to 2.5:1 in the case of OE routing. Apparently, a routing algorithm can have a noticeable impact on the hotspot router's MTTF, and accordingly, it impacts the reliability of the entire chip in the way suggested in Eq. (3).

In the literature, aging-aware adaptive routing algorithms [12,14] have been proposed to slow down the aging of NoCs. The basic idea is to distribute the traffic uniformly across all the routers, to avoid overburdening a few hotspot routers. LAXY [3] is an oblivious routing algorithm that statically partitions the NoCs routers into two classes, and routers in each class adopt their own routing algorithms. Doing so will help balance the network traffic and consequently mitigates routers' aging.

### 2.3. Aging attack on NoCs

Malicious users or intended manufacturers can launch attacks to deliberately accelerate chip aging. There are a few techniques and approaches that are available to achieve accelerated aging. Targeting circuit logic components, Karimi et al. [2] crafted a malicious program that generates identified input patterns to expedite aging in the pipeline stages of a core. Although this type of aging attack can cause a few processors to age prematurely, its effects are still limited due to high degree of redundancy in many-core systems. When a processor core is down, its role can be simply and quickly replaced by many others.

Aiming at the memory hierarchy wear out, Patrick et al. [15] developed an attack that causes inconsistency in nonvolatile flip-flops in the repeating checkpointing process by interrupting the power supply. Wearing out the memory leads to malfunction of the corresponding core, but it still can be solved by task scheduling in NoC.

Unlike processor cores and memory, NoC, as the communication backbone to connect all the processor cores, is a perfect target for aging. Bringing down even a small fraction of the NoC can have devastating effect on the entire chip. Aging the TSV interconnect in NoC has been suggested in [1], while this technique is limited to 3D IC only. A more catastrophic effect can be achieved by aging routers, as malfunction in one router can be amplified by impacting all the processors and the neighboring routers that it directly connects to.

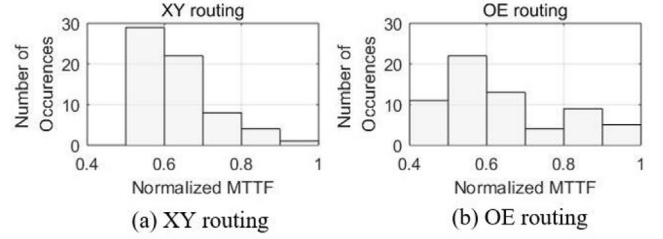


Fig. 3. The routers' MTTFs under two routing algorithms (a) XY and (b) OE routing, respectively.

Since router is an essential component, but happens to be a more vulnerability component in an NoC, this paper focuses on routers considered as the hotspot nodes to be the aging attack targets. As alluded before, the routing algorithms can be explored to either accelerate aging (making most traffic traverse the hotspot node) or decelerate aging (evenly distributing network traffics among all the routers), routing computation of routers can be maliciously elaborated. A manufacturer controls the chip aging by launching this type of aging attack to maximize the profit.

### 2.4. Stealthiness of aging attack

Various denial of service (DoS) attacks targeting NoC routers or links [16,17] have been studied in the literature. These DoS attacks target either the data packet to be delivered directly or the routing paths. In some cases, packets might get dropped, or packet payloads are tampered by a malicious router. In other cases, packets are forced to make illegal routing turns that may get the system into deadlocks. Despite their intended target, these attacks cause traceable harms and damages to the NoC and ultimately the entire chip. For instance, the program may produce wrong results, or the system may come to a sudden halt or an exception is raised. Such manifestations and traces can be explored for the purpose of attack detection and mitigation. In a sharp contrast, none of these effects will be registered in an aging related attack that is found to be much stealthier. As a matter of fact, the aging attack revealed in this paper takes much longer time to be sensed by a product's end user, or even it will not be realized at all throughout the lifetime of a product.

Stationary malfunction launched by the deterministic attack after the warranty arouses suspicion. For example, if each user finds his/her device malfunction just after the warranty expires, they will accuse the manufacturer. In this manner, probabilistic failure caused by aging makes this planned obsolescence attack hard to be detected.

## 3. The manufacturer strategy

When a profit-driven manufacturer needs to develop an aging strategy for its product, a workable profit model is required to calculate profits under different scenarios. As alluded before, it serves the manufacturer's best interest to make sure that the product functions as promised when it is under warranty, and customers are willing to moving to a new version of the product, for the reasons of product malfunction or something else, soon after the warranty expires. To have such a desirable product lifecycle, the manufacturer may have to develop a capability to accelerate and decelerate the aging of its product at different phases of a product's life cycle. In this section, we first present a profit model concerning the refund cost under warranty. To maximize the profit as predicted by this model, aging acceleration and deceleration strategies will be presented, and a product can switch between the two through an aging controller module as described in this section.

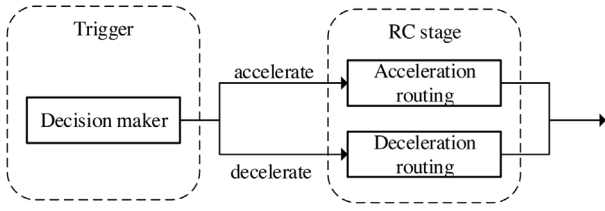


Fig. 4. Architecture of the control module.

### 3.1. The profit model

The profit of the manufacturer for the  $i$ th-version devices can be written as,

$$W_i = (P_i - C_i) \times S_i \quad (4)$$

where  $P_i$ ,  $C_i$ , and  $S_i$  are the price, the cost, and the number of sold copies of the  $i$ th-version devices, respectively. The sales volume  $S_i$  is written as,

$$S_i = \sum_{l=1}^{i-1} \rho_{i-l} \times S_{i-l} + S_0 \quad (5)$$

where  $\rho_{i-l}$  is the probability that customers who bought the  $(i-l)$ th-version of the devices would switch to the new-version, and  $S_0$  is the number of new clients who have never bought any previous version of the product.

Let event  $B$  be the occurrence of an event that a customer buys a new version of the device, and let event  $A$  be the occurrence of an event that a customer's old version device is worn out. In this case,  $\rho_{i-l}$  in Eq. (5) can be further written as,

$$\rho_{i-l} = \rho(B|A) \times \rho(A) + \rho(B|1-A) \times \rho(1-A) \quad (6)$$

where  $\rho(B|A) \times \rho(A)$  is the probability that a customer buys a new version of device given that his/her old-version device malfunctions, and  $\rho(B|1-A) \times \rho(1-A)$  is the probability that a customer buys a new device, even though his/her old-version device still functions.

Taking the warranty into account, one can see that, with the version  $g$  as its latest model, the profit for the  $i$ th-version can be calculated as,

$$W_i = \left\{ \sum_{l=1}^g [p_{Ml} \times x_{i-l} + p_{Wl} \times (1 - x_{i-l})] \times S_{i-l} + S_0 \right\} \times (P_i - C_i) - \sum_{m=1}^w \sum_{n=0}^{w-m} (x_{i-m} \times S_{i-g+n}) \times C_i \quad (7)$$

where  $x_i$  is the failing rate of the  $i$ th-version of the device,  $S_0$  is the number of new customers,  $w$  is the product warranty and  $p_{Ml}$  and  $p_{Wl}$  are the respective  $(i-l)$ th-version device's probabilities,  $\rho(B|A)$  and  $\rho(B|1-A)$  as defined in Eq. (6).

The failing rate  $x_{i-l}$  in Eq. (7) is assumed to follow the Gaussian distribution denoted as  $G(\mu, \sigma^2)$ . Here the mean  $\mu$  is obtained from Eq. (3), and the variance  $\sigma^2$  is a random variable. By setting  $\alpha = 0.5$  as the testing condition,  $x_{i-l}$  is generated by randomly sampling from  $G(\mu, \sigma^2)$ . For the proposed planned obsolescence, the value of  $x_{i-l}$  depends on the triggering condition of aging acceleration.

### 3.2. The aging controller module in NoC

The aging controller module is designed to use router aging acceleration during a time trigger threshold, and router aging deceleration after the time trigger threshold, which is set according to the terms of the warranty agreement (analyzed in Section 5.2.2).

Placed at each router, the control module, shown in Fig. 4, consists of the trigger and the routing computation (RC) submodules. When the product is still under warranty, the routers will adopt a routing strategy

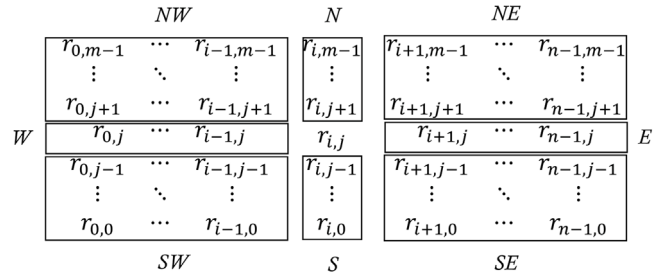


Fig. 5. Network partition.

**Table 1**  
Definition of region partition.

Region	Definition
NW	For each $r_{x,y}$ , $0 \leq x < i, j < y \leq m-1$ .
N	For each $r_{x,y}$ , $x = i, j < y \leq m-1$ .
NE	For each $r_{x,y}$ , $i < x \leq n-1, j < y \leq m-1$ .
W	For each $r_{x,y}$ , $0 \leq x < i, y = j$ .
E	For each $r_{x,y}$ , $i < x \leq n-1, y = j$ .
SW	For each $r_{x,y}$ , $0 \leq x < i, 0 \leq y < j$ .
S	For each $r_{x,y}$ , $x = i, 0 \leq y < j$ .
SE	For each $r_{x,y}$ , $i < x \leq n-1, 0 \leq y < j$ .

that helps decelerate aging. This module continuously compares the trigger threshold with the system clock, and forces routers to switch to a different routing strategy to accelerate aging, once the trigger threshold is reached.

As NoC is the communication infrastructure for high performance many-core chips [18–20], in what follows, we assume that the NoC under attack cannot be powered off when the chip is powered on.

### 4. Routing algorithms

The NoC is assumed to have a mesh topology. Without loss of generality, and for simplicity, a network with  $n \times m$  routers (nodes) can be represented in a matrix format with each entry corresponding to a router, as shown in Fig. 5. Assume  $r_{i,j}$  is the hotspot node and it is not located at the periphery of the network. The network matrix can be partitioned into nine regions with  $r_{i,j}$  at the center and surrounded by other eight regions (defined in Table 1). If the hotspot node,  $r_{i,j}$ , is located at the periphery of the network (i.e.,  $i = 0$ , or  $j = 0$ , or  $i = n-1$ , or  $j = m-1$ ), one or a few regions will have no router.

The same routers can be taken differently when there are multiple hotspot nodes. For instance, if routers  $r_{0,0}$  and  $r_{3,3}$  are the hotspot nodes, then  $r_{1,1}$  falls into region NE of hotspot node  $r_{0,0}$  and into region SW of  $r_{3,3}$ .

Hotspot nodes can be obtained from traffic profiling by the manufacturer. In case that traffic profiles cannot be readily obtained, data traffic can be collected on the fly with the help of system software like operating system, and hotspot nodes, in this case, can be dynamically located as they handle more data traffic than any other routers in the NoC.

#### 4.1. Routing algorithm for aging acceleration

For aging acceleration, even if there are multiple hotspot nodes, we only need to target one single hotspot node, as the chip's lifetime is bounded by the one with the lowest MTTF. Targeting multiple hotspot nodes for aging purpose brings no additional benefit for the sake of aging.

Once the trigger module activates the aging acceleration signal, the RC module selects the aging acceleration routing algorithm to route data packets, which stipulates the packets' routing paths to include the hotspot node. That is, the hotspot node is set as the temporary



destination of a packet, and the packet is first transmitted to this hotspot node by XY routing, after which it will be delivered to the destination node.

As shown in Algorithm 1, the aging acceleration routing algorithm consists of a decision step (lines 1 to 4) and a routing step (line 5). The decision step checks whether a packet can traverse the hotspot node to satisfy three conditions, including minimal routing, turn model, and stealthiness.

To ensure the minimal routing in a network given in Fig. 5, a packet needs to travel along a path such that at every intermediate node, the next node will be the one bringing the packet one hop closer to the destination (line 1).

Following the west-first turn model [21], only the west side of the network participates in the aging acceleration (line 2). That is, the source node of a packet is restricted to locate in the regions of NW, W, SW, N, and S.

A threshold is set for the manufacturer to balance between the effectiveness and the stealthiness of aging acceleration. A packet is forced to pass through the hotspot node only if the threshold is not greater than the Manhattan distance between the source node and the hotspot node (line 3). This approach can help alleviate the congestion around the hotspot node that otherwise can cause serious performance degradation and undermine the attack stealthiness.

When all the above listed conditions are satisfied, the hotspot node is regarded as the temporary destination (line 4). The packet is first routed to the hotspot node by XY routing, and then from the hotspot to the final destination again by XY routing. If a packet is determined not to pass the hotspot node, it will be routed from the source to the destination directly.

#### Algorithm 1: Aging Accelerating Routing Algorithm

---

**Input:**  
*Cur*: The address of the current node.  
*Hot*: The address of the hotspot node.  
*Src*: The address of the source node.  
*Dst*: The address of the destination node.  
**Output:** *Dir*: The output direction of the packet.  
**Result:** Find the direction for the packet path that first travels to the hotspot node, and then to the destination.

---

```

/* Decision module */
1 if (Minimal routing condition is satisfied) and
2 (Src.x ≤ Hot.x) and
3 (|Src.x - Hot.x| + |Src.y - Hot.y| ≤ thr) then
4   Dst ← Hot;
/* Routing module */
5 do XY routing;

```

---

An example is shown in Fig. 6. Here the NoC is a  $7 \times 7$  network, and the destination and the source nodes are (6, 5) and (1, 2), respectively. The current node is marked in gray, and the hotspot node is (5, 4). The threshold is set as 7. When the packet arrives at node (1, 2) in Fig. 6(a), as all the three conditions for aging acceleration are satisfied, the packet will be sent to the hotspot node first. According to the XY routing algorithm, the routing module sets the output direction as East and forwards the packet to node (2, 2); the packet traverses nodes (2, 2), (3, 2), (4, 2), (5, 2), (5, 3), and finally arrives at node (5, 4) in Fig. 6(b). From the hotspot node (5, 4), the packet is routed to its destination node (6, 5) in this case, following the path defined by XY routing.

#### 4.2. Routing algorithm for aging deceleration

For aging deceleration, all the hotspot nodes have to be considered together. Yet the whole chip's lifetime is bounded by the one with the lowest MTTF, and the life time of each individual hotspot node has been extended for the longevity of the chip.

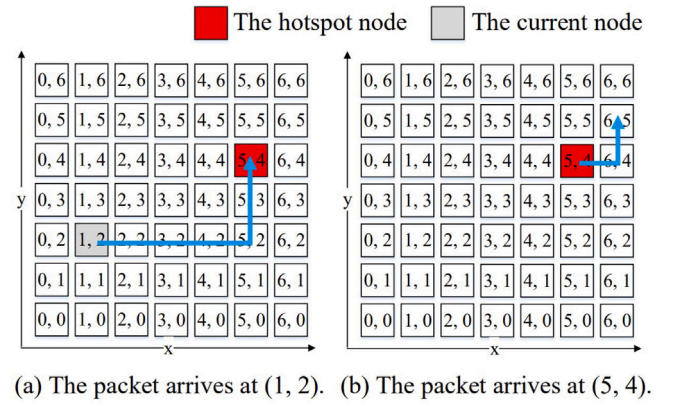


Fig. 6. An example illustrating aging acceleration routing.

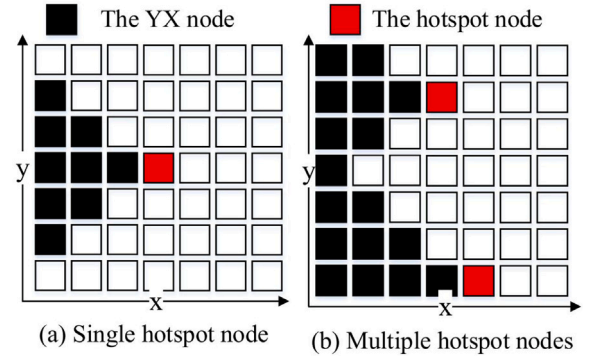


Fig. 7. Examples of the YX region.

Once the trigger module activates the aging deceleration signal, the RC module selects the aging deceleration routing algorithm, which diverts packets to be routed along the paths away from the hotspot nodes.

A specific region that runs YX routing algorithm, named as YX region, is composed of nodes given by Eq. (8), assuming the hotspot node is  $(x_0, y_0)$ . When there are multiple hotspot nodes, the YX region is formed for each hotspot node, as shown in Fig. 7. The YX region forms a triangle shape, and it shall be able to generate more evenly distributed traffic as indicated in [3]. To ensure the routing is deadlock-free, the YX region is formed from only the west of the network, and follows the west-first turn model [21].

$$|y_0 - y| < x_0 - x \quad (8)$$

As shown in Algorithm 2, the aging deceleration routing consists of a decision step (lines 1 to 5) and a routing step (lines 6 to 9). The decision step checks whether the packet is located at the YX region or not (line 1). By applying the west-first turn model, the destination node of a packet is restricted to locate in the regions of NE, E, and SE (line 2).

If both the conditions are satisfied, the YX routing signal is sent to the routing module to make the packet divert from the hotspot node. Otherwise, the routing module directly runs XY routing.

An example is shown in Fig. 8. Here the NoC is a  $7 \times 7$  network, and the destination and the source nodes are (6, 5) and (1, 2), respectively. The current node is marked in gray, and the hotspot node is (5, 4). The YX region is shown in Fig. 8(b). When the packet arrives at node (1, 2) in Fig. 8(a), the packet will follow YX routing, as both conditions for aging deceleration are satisfied. According to the YX routing algorithm, the routing module sets the output direction to be North and forwards the packet to node (1, 3); the packet traverses nodes (1, 3), (1, 4), (1, 5), (2, 5), (3, 5), (4, 5), (5, 5), and finally arrives at node (6, 5).

**Algorithm 2:** Aging Deceleration Routing Algorithm

**Input:**  
*Cur*: The address of the current node.  
*Hot*: The address of the hotspot node.  
*Dst*: The address of the destination node.  
**Output:** *Dir*: The output direction of the packet.  
**Result:** Find the direction for the packet path that bypasses the hotspot node as possible.

```

/* Decision module */
1 if (Cur is located in the YX region) and
2 (Dst.x > Hot.x) then
3   | flag ← 1;
4 else
5   | flag ← 0;
/* Routing module */
6 if flag = 1 then
7   | do YX routing;
8 else
9   | do XY routing;

```

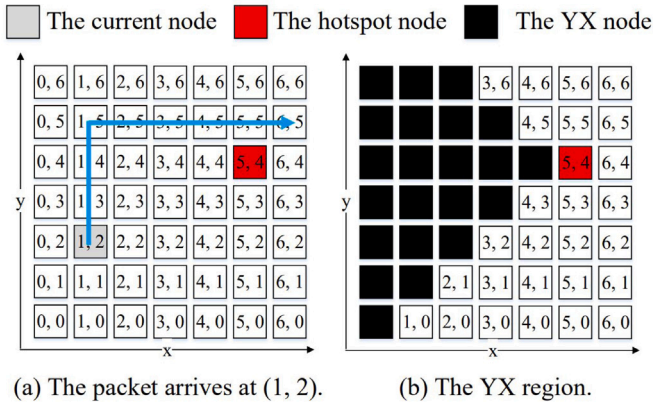


Fig. 8. An example illustrating aging deceleration routing.

**Table 2**  
MTTF model parameters.

Parameter	Value	Description
$b_{NBTI}$		Fitting number of MTTF
$n$	0.166	Time exponent
$E_a$	0.49	Activation energy (eV)
$k$	$1.380649e-23$	Boltzmann's constant (J/°K)
$T$		Temperature (°K)
$a$	0.5	Duty cycle

**5. Experimental evaluation****5.1. Experimental setup**

The parameters in the aging model in Section 2.2 are listed in Table 2. To obtain the probabilities whether the customers will buy the devices under different scenarios or not in Section 3.1, a survey is conducted that each person is asked to answer the questions listed in Table 3. 116 people (college students and faculty members) were surveyed and their ages range from 18 to 36. We apply the statistical data to fit Eq. (7), and the probabilities are also shown in Table 3.

The experiments are simulated using an event-driven many-core simulator [21]. The architecture comes with a shared-memory, and each core has a private L1 cache, and a shared L2 cache bank; all the cores are connected to routers in NoC [22]. The detailed simulator configuration is shown in Table 4. McPAT [23] is also integrated into the

**Table 3**

Survey result and profit model parameters.

Poll Questions		
Will you buy a new version smart phone if it malfunctions in 1/2/3 year/years?		
Will you buy a new version smart phone if your current one is still functional after 1/2/3 year/years?		
Profit model parameters		
Parameter	Value	Description
$p_{M1}$	57.14%	The probability that the customers will buy the devices, knowing it will malfunction in 1 year.
$p_{M2}$	66.67%	The probability that the customers will buy the devices, knowing it will malfunction in 2 years.
$p_{M3}$	80.95%	The probability that the customers will buy the devices, knowing it will malfunction in 3 years.
$p_{W1}$	19.05%	The probability that the customers will buy the devices when it is still working within 1 year.
$p_{W2}$	38.09%	The probability that the customers will buy the devices when it is still working within 2 years.
$p_{W3}$	14.29%	The probability that the customers will buy the devices when it is still working within 3 years.

**Table 4**

Configurations of the simulations.

Configuration of the many-core simulator for trace extraction	
Number of processors	64 (MIPS ISA 32 compatible)
Fetch/Decode/Commit size	4 / 4 / 4
ROB size	64
L1 D cache (private)	16 KB, two-way, 32B line, two cycles, two ports, dual tags
L1 I cache (private)	32 KB, two-way, 64B line, two cycles
L2 cache (shared) MESI protocol	64 KB slice/node, 64B line, six cycles, two ports
Main memory size	2 GB, latency 200 cycles
Frequencies available	1 GHz, 800 MHz, 500 MHz, 330 MHz
On-chip network parameters	
NoC size	8 × 8
Number of routers	64
NoC flit size	72-bit
NoC latency	Router 1 cycle, link 1 cycle
NoC VC number	1
NoC input buffer size	12
NoC output buffer size	12

**Table 5**

Benchmarks used in the simulation.

PARSEC	Blackscholes, bodytrace, canneal, ferret, fluidanimate, streamcluster, vips, x264
SPLASH-2	Raytrace

simulator to measure the power consumption of each router, followed by using HotSpot for computing the temperature. MTTF is evaluated by the aging model given in Eq. (3). The simulation is performed using both random benchmarks and a few real benchmarks. The random benchmarks are generated randomly, while the real benchmarks used for performance evaluation are shown in Table 5, which are selected from PARSEC [24] and SPLASH-2 [25].

Fig. 9 illustrates the different configurations of the hotspot nodes and the YX regions for different simulation scenarios. For the random benchmarks, the hotspot node is generally considered as the central node of the network, which is typically the most vulnerable component of the chip. The YX region is set in the west of the hotspot node, and the west-first turn model [21] is adopted under this scenario. For the real benchmarks, the memory controllers of the simulator are connected with the routers (2, 0), (5, 0), (2, 7) and (5, 7). As the profiling data from pre-simulation indicate (2, 0) is the most congested node for any real benchmarks, it is set as the only hotspot node. The YX region is correspondingly set on its east for maximizing aging deceleration effect, and the negative-first turn model [21] is adopted under this scenario.

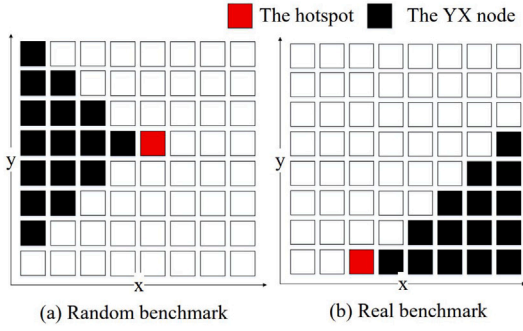


Fig. 9. The configuration of the hotspot nodes and the YX regions.

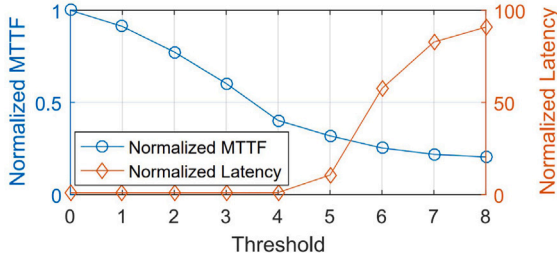


Fig. 10. Normalized MTTF and latency with respect to threshold.

Different benchmarks still lead to the same hotspot node under same CMP configuration. Thus, the critical node can be set as the default target from the pre-simulation.

The threshold needed in the aging acceleration routing algorithm is predetermined to balance the aging effect and latency. Fig. 10 shows the impact of the threshold on the MTTF and latency. One can see that the latency soars as the threshold is greater than 4. In the following experiment, the threshold is thus set to be 4.

## 5.2. Experimental results

As alluded in Section 2.4, stealthiness is so critical to sustain and thus ensure the success of any ongoing planned obsolescence attack, which is so different from other DoS attacks that emphasizes timing error for effectiveness. Network throughput and latency would give a clear indication of stealthiness, and the effectiveness of the proposed attack is measured by MTTF, which is of no concern to other DoS attacks.

In what follows, we will first present the results related to the effectiveness and stealthiness evaluation of the proposed aging attack in Section 5.2.1. The profit evaluation results are reported and analyzed in Section 5.2.2, and finally we will examine the overheads in Section 5.2.3.

### 5.2.1. MTTF and performance evaluation

The results of the simulation implemented running random traffic are first analyzed. The temperatures of the proposed two routing algorithms are compared against XY and OE routing algorithms. Fig. 11(a) shows that the proposed aging acceleration routing algorithm can increase the chip temperature by 17.17 °C and 14.66 °C higher than XY and OE routing algorithms, respectively. Fig. 11(b) shows that the proposed aging deceleration routing algorithm can help reduce the chip temperature by 4.91 °C and 7.42 °C over XY and OE routing algorithms, respectively.

The normalized traffic volume passing through hotspot nodes of the two proposed routing algorithms are shown in Fig. 12(a). The proposed aging acceleration routing algorithm increases the traffic volume of the

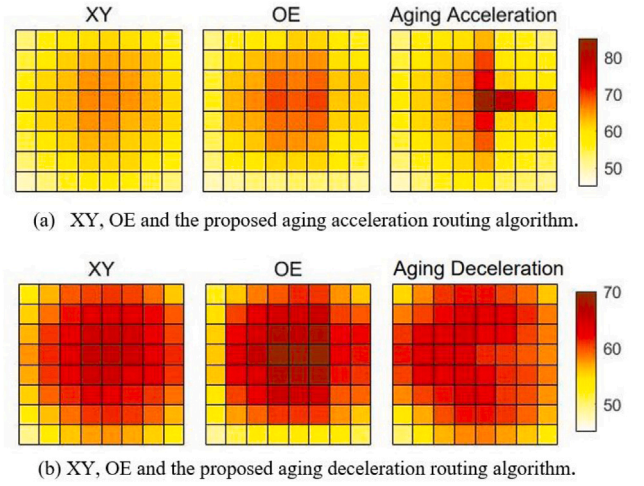


Fig. 11. The temperature distribution of NoCs with different routing algorithms.

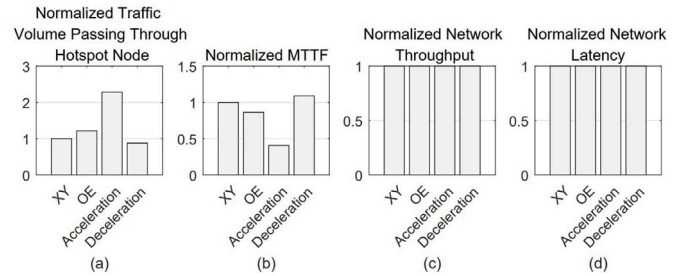
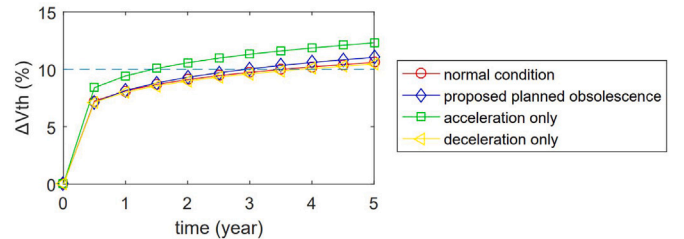


Fig. 12. (a) The normalized traffic volumes passing through hotspot nodes, (b) the normalized MTTFs, (c) the normalized network throughputs, and (d) the normalized network latencies of NoCs with different routing algorithms running random benchmark.

Fig. 13. The variations of  $\Delta V_{th}$  over time.

hotspot node by 128.22% and 106.79% over XY and OE routing algorithms, respectively. The proposed aging deceleration routing algorithm decreases the traffic volume of hotspot node by 12.33% and 33.76% over XY and OE routing algorithms, respectively.

The normalized MTTF results of the two proposed routing algorithms are shown in Fig. 12(b). The proposed aging acceleration routing algorithm downgrades the MTTF by 59.35% and 52.89% over XY and OE routing algorithms, respectively. The proposed aging deceleration routing algorithm improves the MTTF by 8.88% and 26.19% over XY and OE routing algorithms, respectively.

The normalized network throughput and latency results of the two proposed routing algorithms are shown in Fig. 12(c) and (d), respectively. The proposed aging acceleration routing algorithm and the proposed aging deceleration routing algorithm have almost the same throughput and latency as XY and OE routing algorithms. Therefore, the attack is stealthy, *i.e.*, no salient performance degradation can be observed by users.



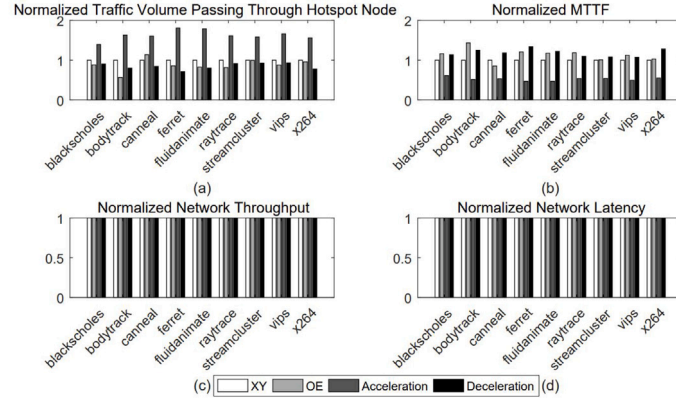


Fig. 14. (a) The normalized traffic volumes passing through hotspot nodes, (b) the normalized MTTFs, (c) the normalized network throughputs, and (d) the normalized network latencies of NoCs with different routing algorithms running different real benchmarks.

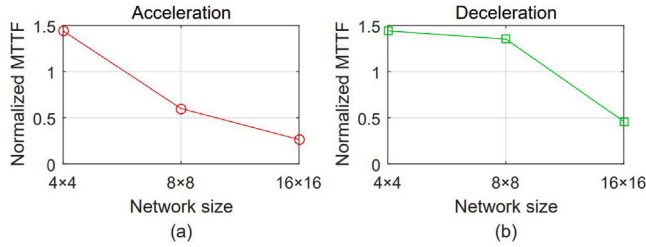


Fig. 15. The normalized MTTF results of the proposed (a) aging acceleration and (b) aging deceleration routing algorithms vs. the network size.

The variations of  $\Delta V_{th}$  (i.e., change of transistor threshold voltage) over time are evaluated for different scenarios, that is, normal condition (without any attack), the proposed planned obsolescence attack (deceleration first and acceleration after the trigger threshold), acceleration only, and deceleration only schemes, as shown in Fig. 13. In this evaluation, the chip can be considered as faulty when  $\Delta V_{th}$  exceeds 10%. The NoC under the proposed planned obsolescence malfunctions 14.51% and 23.79% faster than the NoC under normal condition and deceleration only, respectively. Compared to the acceleration only case, the proposed planned obsolescence slows down the aging by 48.95%.

Fig. 14 shows the results of the proposed two routing algorithms with XY and OE routing algorithms running the real benchmarks. The normalized traffic volume passing through hotspot nodes of the two proposed routing algorithms are shown in Fig. 14(a). The proposed aging acceleration routing algorithm increases the average traffic volume of hotspot node by 62.88% and 85.07% over XY and OE routing algorithms, respectively. The proposed aging deceleration routing algorithm decreases the average traffic volume of hotspot node by 15.41% and 3.98% over XY and OE routing algorithms, respectively.

The normalized MTTF results of the two proposed routing algorithms are shown in Fig. 14(b). The proposed aging acceleration routing algorithm downgrades MTTF by 47.54% and 53.64% on average over XY and OE routing algorithms, respectively. The proposed aging deceleration routing algorithm improves MTTF by 18.46% and 4.69% on average over XY and OE routing algorithms, respectively.

The normalized network throughput and latency results of the two proposed routing algorithms are shown in Fig. 14(c) and (d), respectively. The proposed aging acceleration and the aging deceleration routing algorithms have almost the same throughput and latency as XY and OE routing algorithms, as a result of the two factors. First, both the aging acceleration and deceleration algorithms fall into the family of minimal-path routing, meaning that packets follow the shortest path, linking the source to the destination. Second, since PARSEC and

Table 6

Parameters and variables of the profit model.

Profit model parameters		
Parameter	Value	Description
$P$ (USD)	8500	The price of the device
$C$ (USD)	3000	The cost of the device
$S$	250 000	The number of the old customers who have bought the devices within the last $g$ versions
$S_0$	$0.4 \times S$	The number of the new customers who have not bought the devices within the last $g$ versions
$w$ (year)	2	The warranty of the device
$g$ (year)	3	The generations considered in the model
$\sigma^2$	0.25	The variance that influences the failing rate $x_{i-j}$
The range of profit model variables		
Parameter	Range	
$S$	(100 000, 400 000)	
$P$ (USD)	(5000, 10 000)	
$C$ (USD)	(1000, 3500)	
$\sigma^2$	(0, 3)	
$w$ (year)	(0, 2)	

SPLASH-2 applications have light traffic loads [26], the data traffic will not cause congestion in the NoC.

In Fig. 15, the normalized MTTFs of the networks running proposed aging acceleration and deceleration routing algorithms (with respect to that of the case featuring an  $8 \times 8$  network with XY routing algorithm) are obtained for various network sizes. One can see that as the network size scales up, the minimal MTTFs of the NoC running both acceleration and deceleration routing algorithms decrease. This is because in a larger network, more traffic tends to flow through the hotspot nodes making them age faster. When the network size is  $8 \times 8$ , both the acceleration and deceleration effect reach the peak, 40.006% greater and 35.19% less than XY routing, respectively.

### 5.2.2. Profit evaluation

Table 6 lists the configuration of parameters in the profit model in Eq. (7), using the probabilities in Table 3. The profits are evaluated for different scenarios, that is, normal condition (without any attack), the proposed planned obsolescence attack, acceleration only (with a planned obsolescence attack using only the aging acceleration routing in Section 4.1), and deceleration only (with a planned obsolescence attack using only the aging deceleration routing in Section 4.2) schemes.

The trigger threshold when the aging acceleration routing algorithm launches, referred in Section 3.2, is analyzed and the relationship between the trigger threshold and the manufacturer profit is shown in Fig. 16. The profits are normalized with respect to that with the case



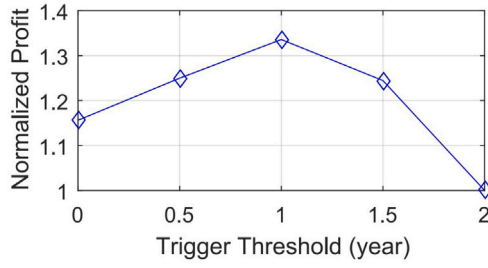


Fig. 16. The relationship between the trigger threshold and the normalized manufacturer profits.

with the configuration in Table 6. From Fig. 16, one can see that when the trigger threshold is set to be 1 year, the normalized manufacturer profit reaches the maximum. In the following evaluation, the trigger threshold is configured as 1 year.

Fig. 17 shows the profits when varying the sales volume, the price, the cost, the variance, and the warranty. These profits are normalized with respect to the profit of case as summarized in Table 6.

From Fig. 17(a), one can see that the profit with the proposed attack increases at a much faster rate than the other schemes under different sales numbers. When the sales volume is 400 000, the profit of the proposed planned obsolescence attack is 15.54%, 25.69%, and 53.36% higher than that of the normal condition, acceleration only, and deceleration only schemes, respectively. The increased profit can be attributed to the combined effect that the proposed attack helps reduce refund and at the same time increases the sales volume to new customers. If a manufacturer only engages in aging acceleration only scheme, it actually loses money to the normal condition (*i.e.*, not engaging in such activity), if when refunding is factored in to observe the warranty.

From Fig. 17(b), one can see that, for the price of \$10,000, the profit of the proposed planned obsolescence attack is 17.69%, 12.48%, and 56.56% higher than the normal condition, acceleration only, and deceleration only schemes, respectively.

When the cost is \$3,500, the profit of the proposed planned obsolescence attack is 12.68%, 50.17%, and 49.12% higher than the normal condition, acceleration only, and deceleration only schemes, respectively, as shown in Fig. 17(c). The profit with the proposed attack is 32.60% and 77.02% higher than the acceleration only and deceleration only schemes, respectively when the variance converges towards 0 (Fig. 17(d)). The curves of all the schemes tend to be the same as the variance increases.

From Fig. 17(e), one can see that without taking the warranty into account (when the warranty is 0), the profit of the acceleration only scheme is higher than the others, and the profit with the acceleration only scheme decreases as the warranty increases. When the warranty is 2 years, the profit is 8.07% and 20.44% lower than the normal condition and the proposed planned obsolescence attack, respectively. The profit of the proposed planned obsolescence attack is 15.54%, 25.69%, and 53.36% higher than the normal condition, acceleration only, and deceleration only schemes, respectively.

From Fig. 17(f), one can see that the profit at the presence of the proposed attack increases as the network size increases. Among these four schemes, the proposed planned obsolescence attack leads to the maximal profit in both the 8 × 8 and 16 × 16 networks.

### 5.2.3. Overhead analysis

The hardware cost of the proposed router is analyzed from the synthesis result reported by Synopsys Design Compiler with a TSMC 45 nm CMOS library. From DSENT [27], the XY router with the configuration in Table 4 with 45 nm CMOS technology consumes 16.6 mW power and has an area of 57 530  $\mu\text{m}^2$ . The power consumption and

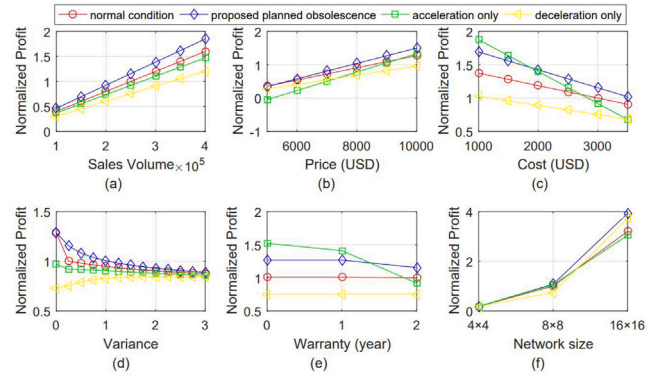


Fig. 17. Normalized manufacturer profits under different scenarios by varying (a) the sales volume, (b) the price, (c) the cost, (d) the variance, (e) the warranty, and (f) the network size.

area of the proposed router is 16.7 mW and 57 664  $\mu\text{m}^2$ . Therefore, the power consumption and area overhead of the proposed router are fairly modest, only 0.60% and 0.23% higher than the original router, respectively.

## 6. Conclusion

In this paper, we detailed a planned obsolescence attack that targets the hotspot routers, the most vulnerable part of NoC-based many-core chips. In particular, we added the product warranty into the aging model to reveal how a manufacturer can maximize its profit. In specific, the planned aging can be achieved with the two proposed routing algorithms: one for accelerated aging when the warranty expires, and one for decelerated aging when the warranty is still in effect. Experiments have shown that the former algorithm reduces the MTTF of the chip by about 47.54% and the latter algorithm improves the MTTF by about 18.46%. The profit from the proposed planned obsolescence is 15.54%, 25.69%, and 53.36% higher than that from the normal condition, acceleration only, and deceleration only schemes, respectively. This study clearly shows that the proposed planned obsolescence attack secretly causes more economic losses to customers, which needs to be balanced out with appropriate countermeasure yet to be developed.

### Declaration of competing interest

The authors declare that they have no known competing financial interests or personal relationships that could have appeared to influence the work reported in this paper.

### References

- [1] S. Das, K. Basu, J.R. Doppa, P.P. Pande, R. Karri, K. Chakrabarty, Abetting planned obsolescence by aging 3D networks-on-chip, in: IEEE/ACM Int'l Symp. Networks-on-Chip, 2018, pp. 76–83.
- [2] N. Karimi, X. Wang, MAGIC: Malicious aging in circuits/cores, ACM Trans. Archit. Code Optim. 12 (1) (2015) 5:1–5:25.
- [3] N. Rohbani, Z. Shirmohammadi, M. Zare, S. Miremadi, LAXY: A location-based aging-resilient xy-yx routing algorithm for network on chip, IEEE Trans. Comput. Aided Des. Integr. Circuits Syst. 36 (10) (2017) 1725–1738.
- [4] H. Kim, A. Vitkovskiy, P.V. Gratz, V. Soteriou, Use it or lose it: Wear-out and lifetime in future chip multiprocessors, in: IEEE/ACM Int'l Symp. Microarchitecture, 2013, pp. 136–147.
- [5] H. Amrouch, P. Krishnamurthy, N. Patel, J. Henkel, R. Karri, F. Khorrami, Special session: Emerging (un-)reliability based security threats and mitigations for embedded systems, in: IEEE Int'l Conf. Compilers Architectures Synthesis Embedded Systems, 2017, pp. 1–10.
- [6] G. Chen, M.F. Li, C.H. Ang, J.Z. Zheng, D.L. Kwong, Dynamic NBTI of p-MOS transistors and its impact on MOSFET scaling, IEEE Electron Device Lett. 23 (12) (2002) 734–736.

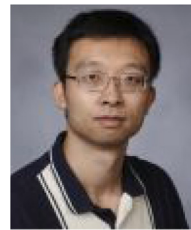
- [7] A.T. Krishnan, V. Reddy, S. Chakravarthi, J. Rodriguez, S. John, S. Krishnan, NBTI impact on transistor and circuit: models, mechanisms and scaling effects, in: IEEE Int'l Electron Devices Meeting, 2003, pp. 14.5.1–14.5.4.
- [8] M. Wang, M. Peng, L. Ji, H. Huang, S. Chen, S. Wang, H. Hsu, W. Liao, C. Liu, Strained pMOSFETs with SiGe channel and embedded SiGe source/drain stressor under heating and hot-carrier stresses, in: IEEE Int'l Symp. Next-Generation Electronics, 2013, pp. 371–374.
- [9] D.M. Ancajas, J.M. Nickerson, K. Chakraborty, S. Roy, HCI tolerant noc router microarchitecture, in: ACM/EDAC/IEEE Design Automation Conf., 2013, pp. 1–10.
- [10] K. Bhardwaj, K. Chakraborty, S. Roy, An MILP-based aging-aware routing algorithm for NoCs, IEEE Des. Autom. Test Exhibition (2012) 326–331.
- [11] Y. Lu, L. Shang, H. Zhou, H. Zhu, F. Yang, X. Zeng, Statistical reliability analysis under process variation and aging effects, in: ACM/EDAC/IEEE Design Automation Conf., 2009, pp. 514–519.
- [12] L. Wang, X. Wang, T. Mak, Adaptive routing algorithms for lifetime reliability optimization in network-on-chip, IEEE Trans. Comput. 65 (9) (2016) 2896–2902.
- [13] G.M. Chiu, The odd-even turn model for adaptive routing, IEEE Trans. Parallel Distrib. Syst. 11 (7) (2000) 729–738.
- [14] K. Bhardwaj, K. Chakraborty, S. Roy, Towards graceful aging degradation in NoCs through an adaptive routing algorithm, in: ACM/EDAC/IEEE Design Automation Conf., 2012, pp. 382–391.
- [15] P. Cronin, C. Yang, Y. Liu, Reliability and security in non-volatile processors, two sides of the same coin, in: IEEE Computer Society Annual Symp. Very Large Scale Integration, 2018, pp. 112–117.
- [16] Y. Zhao, X. Wang, Y. Jiang, L. Wang, M. Yang, A.K. Singh, T. Mak, On hardware-Trojan-assisted power budgeting system attack targeting many core systems, J. Syst. Archit. 109 (3) (2020) 1–11.
- [17] L. Daoud, N. Rafla, Analysis of black hole router attack in network-on-chip, in: IEEE Int'l Symp. Circuits and Systems, 2019, pp. 69–72.
- [18] Y. Chou, S. Liu, E. Chung, J. Gaudiot, An energy and performance efficient DVFS scheme for irregular parallel divide-and-conquer algorithms on the intel SCC, IEEE Comput. Archit. Lett. 13 (1) (2014) 13–16.
- [19] A. Pellegrini, N. Stephens, M. Bruce, Y. Ishii, J. Pusdesris, A. Raja, C. Abernathy, J. Koppalanil, T. Ringe, A. Tummala, J. Jalal, M. Werkheiser, A. Kona, The Arm Neoverse N1 platform: building blocks for the next-gen cloud-to-edge infrastructure soc, IEEE Micro 40 (2) (2020) 53–62.
- [20] Arteris announces Ncore cache-coherent interconnect, 2016, [Online]. Available: <https://www.anandtech.com/show/10339/arteris-announces-ncore-cache-coherent-interconnect>.
- [21] N.E. Jerger, L.S. Peh, On-chip networks, in: Synth. Lect. Computer Architecture, Morgan & Claypool press, 2009.
- [22] X. Wang, M. Yang, Y. Jiang, P. Liu, M. Daneshmand, M. Palesi, T. Mak, On self-tuning networks-on-chip for dynamic networkflow dominance adaptation, ACM Trans. Embedded Comput. Syst. 13 (2) (2014) 73:1–21.
- [23] A. Tang, Y. Yang, C. Lee, N.K. Jha, McPAT-PVT: Delay and power modeling framework for FinFET processor architectures under PVT variations, IEEE Trans. Very Large Scale Integr. Syst. 23 (9) (2015) 1616–1627.
- [24] C. Bienia, S. Kumar, J.P. Singh, K. Li, The PARSEC benchmark suite: Characterization and architectural implications, in: IEEE Int'l Conf. Parallel Architectures and Compilation Techniques, 2008, pp. 72–81.
- [25] S.C. Woo, M. Ohara, E. Torrie, J.P. Singh, A. Gupta, The SPLASH-2 programs: Characterization and methodological considerations, in: IEEE Int'l Symp. Computer Architecture, 1995, p. 24, no. 36.
- [26] R. Hesse, J. Nicholls, N.E. Jerger, Fine-grained bandwidth adaptivity in networks-on-chip using bidirectional channels, in: IEEE/ACM Int'l Symp. Networks-on-Chip, 2012, pp. 132–141.
- [27] C. Sun, C.O. Chen, G. Kurian, L. Wei, J. Miller, A. Agarwal, L. Peh, V. Stojanovic, DSENT – A tool connecting emerging photonics with electronics for opto-electronic networks-on-chip modeling, in: IEEE/ACM Int'l Symp. Networks-on-Chip, 2012, pp. 201–210.



**Yinyuan Zhao** is an undergraduate student in the School of Software Engineering, South China University of Technology. His research interests include networks-on-chip architecture and hardware security.



**Xiaohang Wang** received the B.Eng. and Ph.D. degree in communication and electronic engineering from Zhejiang University, in 2006 and 2011. He is currently an associate professor at South China University of Technology. He was the receipt of PDP 2015 and VLSI-SoC 2014 Best Paper Awards. His research interests include many-core architecture, power efficient architectures, optimal control, and NoC-based systems.



**Yingtao Jiang** joined the Department of Electrical and Computer Engineering, University of Nevada, Las Vegas in Aug. 2001, upon obtaining his Ph.D. degree in Computer Science from the University of Texas at Dallas. He has been a full professor since July 2013 at the same university, and now assumes the role of associate dean of College of Engineering. His research interests include algorithms, computer architectures, VLSI, networking, nano-technologies, etc



**Liang Wang** received the BEng and M.Sc. degrees in electronics engineering from the Harbin Institute of Technology, China, in 2011 and 2013, respectively, and the Ph.D. degree in computer science and engineering from the Chinese University of Hong Kong, Hong Kong, in 2017. He is currently an assistant professor with the School of Computer Science and Engineering, Beihang University, China. He was a postdoctoral research fellow in Institute of Microelectronics, Tsinghua University, China during 2017 and 2020. His research interests include power-efficient and reliability-aware design for network-on-chip, and many-core system.



**Amit Kumar Singh** received the B.Tech. degree in Electronics Engineering from Indian Institute of Technology (Indian School of Mines), Dhanbad, India, in 2006, and the Ph.D. degree from the School of Computer Engineering, Nanyang Technological University (NTU), Singapore, in 2013. He was with HCL Technologies, India for year and half before starting his Ph.D. at NTU, Singapore, in 2008. He worked as a post-doctoral researcher at National University of Singapore (NUS) from 2012 to 2014 and at University of York, UK from 2014 to 2016. Currently, he is working as senior research fellow at University of Southampton, UK. His current research interests include system level design-time and run-time optimizations of 2D and 3D multi-core systems with focus on performance, energy, temperature, and reliability. He has published over 45 papers in the above areas in leading international journals/conferences.



**Letian Huang** received the M.S. and Ph.D. degrees in communication and information system from the University of Electronic Science and Technology of China (UESTC), Chengdu, China, in 2009 and 2016, respectively. He is an Associate Professor with UESTC. His scientific work contains more than 40 publications, including book chapters, journal articles, and conference papers. His research interests include heterogeneous multicore system-on-chips and network-on-chips.



**Mei Yang** received her Ph.D. in Computer Science from the University of Texas at Dallas in Aug. 2003. She has been a full professor in the Department of Electrical and Computer Engineering, University of Nevada, Las Vegas since 2016. Her research interests include computer architectures, networking, and embedded systems.